ELSEVIER

PII: S0032-3861(97)00002-5

Polymer Vol. 38 No. 19, pp. 4863–4871, 1997

0032-3861/97/$17.00+0.00

Reaction of poly(vinyl alcohol) and dialdehydes during gel formation probed by ^{1}H n.m.r.—a kinetic study

E. W. Hansen* and K. H Holm
SINTEF Applied Chemistry, PO Box 124 Blindern, N-0314 Oslo, Norway

and D. M. Jahr, K. Olafsen and Aa. Stori
SINTEF Materials Technology, PO Box 124 Blindern, N-0314 Oslo, Norway
(Received 15 May 1996)

Proton n.m.r. has been used to study the reaction between poly(vinyl alcohol) (PVA) and two different dialdehyde crosslinkers during gel formation (gels for improved oil recovery applications). The rate of formation of covalent bonds between PVA and glutaraldehyde in acidic saline water solutions was found to be of first order with respect to both the H^+ concentration and the formal dialdehyde concentration. The activation energy was found to increase with increasing dialdehyde concentration and increasing pH (3.2–4.7). The corresponding reaction rate of formation of covalent bonds between PVA and butenedial in the PVA/2,5-dimethoxy-2,5-dihydrofuran system at the same pH and temperature was found to be an order of magnitude less. Also, the activation energy was higher by approximately 50% as compared with the PVA/glutaraldehyde system. Possible reaction pathways for the generation of PVA–dialdehyde gels are discussed.

(Keywords: poly(vinyl alcohol); 2,5-dimethoxy-2,5-dihydrofuran; glutaraldehyde)

INTRODUCTION

Polymer gels can be used in order to improve the oil recovery from an oil reservoir[1]. In order to obtain a driving force in oil production, water can be injected through an injection well, and the oil is subsequently forced towards a production well. The injection water tends to follow the zones of the reservoir with the highest permeability and may thus by-pass the oil bearing zones. In this case a polymer gel can be used in order to block the zones of high permeability so that the injection water is diverted towards the oil containing zones with lower permeability.

A polymer gel in this case usually consists of 0.5 to 3 wt% crosslinked polymer in sea water. Probably the most common gel system used for oil recovery applications is partially hydrolysed polyacrylamide (HPAm) crosslinked with Cr^{3+} ions. However, Cr^{3+} is not a favourable crosslinker from an environmental point of view. Poly(vinyl alcohol) (PVA) crosslinked with dialdehydes should represent a more environmentally acceptable system than HPAm/Cr^{3+}.

For practical use it is important to be able to control the rate of gel formation so the gel does not form too fast or too slowly. The most important parameters for gel formation in an oil reservoir are concentrations of polymer and crosslinker, pH, salinity of sea water and temperature. For laboratory studies of gel formation in bulk, different methods have been described, such as simple visual inspection[2], viscometry[3] and dynamic mechanical measurements[4]. Nuclear magnetic resonance (n.m.r.) has also been used in some cases in order to study gel formation of, e.g. HPAm/Cr^{3+} and xanthan/Cr^{3+} [5–8]. However, to our knowledge ^{1}H n.m.r. studies on the kinetics of the reaction between PVA and dialdehyde in aqueous solution have not previously been reported.

The reason for using n.m.r. to study the reaction between PVA and dialdehyde is that a spectroscopic technique should give relevant information about chemical reaction mechanisms and the kinetics for the reactions; such information is not possible to obtain, e.g. viscometry or dynamic mechanical measurements. In this introductory study the reaction between PVA and two different dialdehyde crosslinkers have been studied as a function of temperature, crosslinker concentration and pH (variables of relevance for gel formation in an oil reservoir).

EXPERIMENTAL

Materials

The reagents used in this study were Floperm 665 P (PVA) from OFPG Inc., Floperm 665 X1 (25% glutaraldehyde in water) from OFPG Inc., and 2,5-dimethoxy-2,5-dihydrofuran (DHF, mixture of *cis* and *trans* isomers) from Fluka.

For pH adjustment of gel forming solutions, two different buffers were used: phosphoric acid/sodium dihydrogen phosphate (pH 3.2) and citric acid/disodium phosphate (pH 4.7); NaCl was added to the buffer salt solutions to give a total ionic strength of 0.475, which is comparable to that of sea water. All chemicals were used as received without further purification.

* To whom correspondence should be addressed

Method

The ^{1}H n.m.r. measurements were performed using a Varian VXR spectrometer operating at 300 MHz proton resonance frequency. When using water as a solvent the ratio of the intensity of the water peak and the typically much smaller peak intensities originating from the solute molecules might be much larger than the dynamic range determined by the analogue-to-digital converter (ADC), and results in severe difficulties in detecting the solute molecules[9]. In order to overcome this obstacle the solvent peak was suppressed by applying a so-called 1331 pulse sequence[10]. The disadvantage of this experimental approach, which it shares with other techniques, is a non-uniform 'excitation' of the different resonance peaks. A quantitative comparison between different regions of the spectrum is thus difficult and needs some tedious calibration procedures. However, as will become clear later in this text, this has no significance to the kinetic results presented in this work. Because the description of the solvent suppression technique would become rather tedious and technical we do not discuss it here; interested readers may consult ref. 10.

If not otherwise stated in the text the samples were run within the n.m.r. magnet *in situ* using a sweep width of 6 kHz and an acquisition time of 1 s. The number of transients were dependent on the actual sample under investigation and set to between 64 and 256 scans. The free induction decay was stored in a double precision mode and Fourier transformed after multiplication by an exponential function of time constant equal to 0.06–0.3 s to improve the signal-to-noise ratio. The final spectrum was baseline corrected using a second order polynomial. The area (intensity) of the region of interest was measured by digital integration. The estimated uncertainty of the integral is less than 5% (relative). The temperature was set to a fixed value within ±1°C.

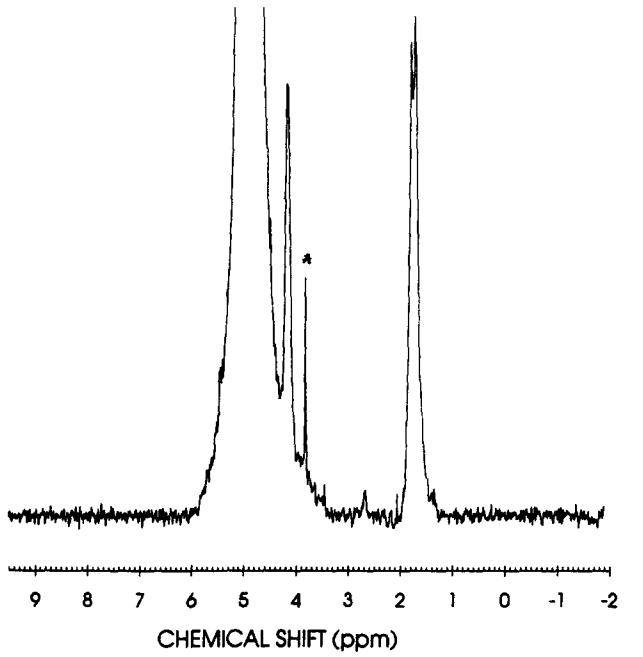

Figure 1 ^{1}H n.m.r. spectrum of 2 wt% PVA in water at room temperature

RESULTS AND DISCUSSION

PVA and glutaraldehyde

Figure 1 shows the ^{1}H n.m.r. spectrum of 2 wt% PVA in water at room temperature. The main peak in the spectrum at $\delta = 4.9$ ppm corresponds to the solvent water protons while the two main peaks from PVA have resonances at $\delta = 1.7$ ppm (-C<u>H</u>$_2$-CHOH-) and $\delta = 4.2$ ppm (-CH$_2$-C<u>H</u>OH-), respectively. The -O<u>H</u> protons in PVA exchange fast with the solvent water protons and causes this peak to coalesce with the solvent water peak. The additional small peak (*) in the spectrum has not been assigned and is tentatively assumed to be a contaminant. Anyway, the intensity of this peak does not change during the reaction with aldehyde. It is worth noting that the chemical shift of the solvent water peak decreases with increasing temperature due to a destruction of hydrogen bonds which results in a coalescence of the solvent peak and the methine proton peak in PVA. This 'fusion' of peaks starts at a temperature above approximately 60°C.

The ^{1}H n.m.r. spectrum at room temperature of glutaraldehyde (25% Floperm in water), which has a simple formal structure of HOC-CH$_{2(a)}$CH$_{2(c)}$CH$_{2(a)}$-COH, is shown in *Figure 2A* and suggests that the structure of the dialdehyde in water is much more complex than initially anticipated. The aldehyde protons

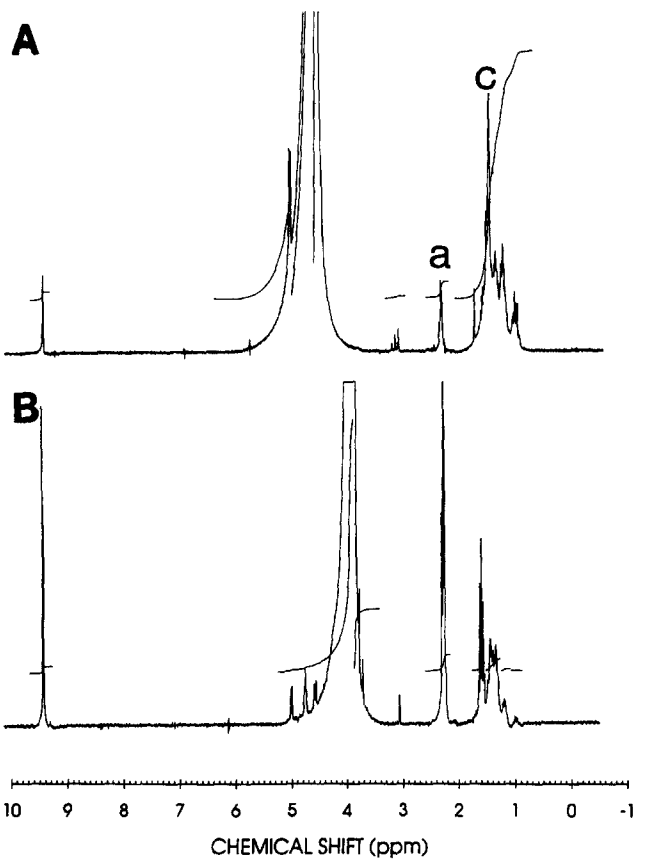

Figure 2 ^{1}H n.m.r. spectrum of glutaraldehyde (25 wt% in water) at (A) 20°C and (B) 80°C

are assigned to the resonance peak at $\delta = 9.4$ ppm, and the triplet and quintet peaks at $\delta = 2.3$ ppm and $\delta = 1.6$ ppm are assigned to the methylene protons *a* and *c* in *Figure 2A*, respectively. The coupling between the aldehyde proton and the nearest methylene protons is probably too small ($J \approx 2$ Hz) compared to the width of the resonance peak to be discerned. However, a significant

part of the intensity distribution is found in the range $\delta = 0.8$–1.3 ppm and is tentatively assumed to be caused by polymerization products of the aldehyde. Additional peaks can be observed around 5 ppm and are probably originating from hydrated species. The monomer concentration of glutaraldehyde at room temperature is estimated to be approximately 20% and increasing to about 70% at 84°C as can be seen from the ^{1}H n.m.r. spectrum in *Figure 2B*, which resembles more the spectrum of monomer dialdehyde. It is well known that the degree of polymerization of an aldehyde decreases with increasing temperature[11]. A mixture of dialdehyde and PVA will thus give rise to a rather complex spectrum with severe overlap of peaks.

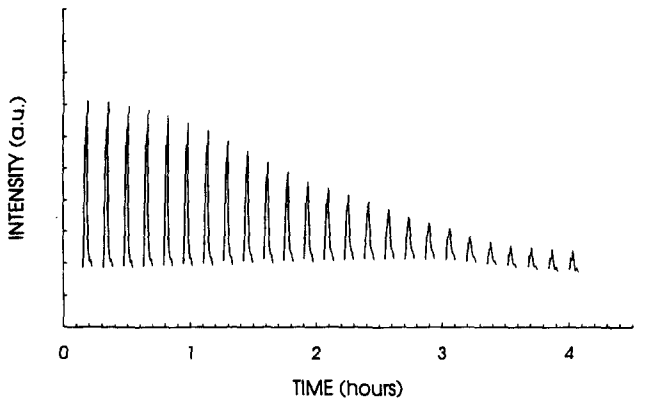

Figure 3 ^{1}H n.m.r. spectrum of the aldehyde peak ($\delta = 9.4$ ppm) *versus* time of a 2 wt% PVA + 5 mM glutaraldehyde at 70°C and pH 3.2

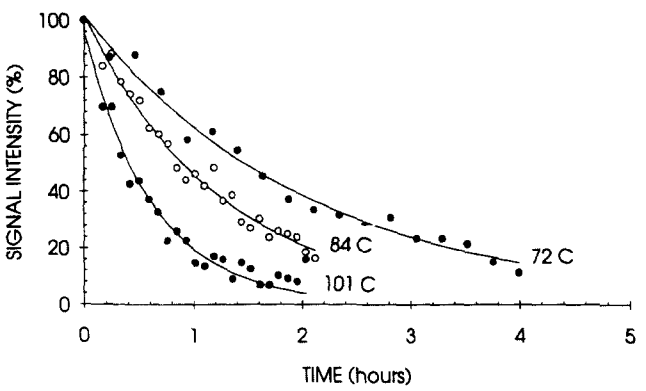

Figure 4 Intensity (area) of the aldehyde peak ($\delta = 9.4$ ppm) *versus* time at three different temperatures. The solid curves represent non-linear least squares fit of a single exponential function, equation (1b), to the observed data

However, in spite of the apparent spectral complexity the aldehyde proton peak shows a decay with time when mixed with PVA at a certain pH and temperature. This is illustrated in *Figure 3* for a system studied at 72°C containing 2 wt% PVA and 5 mM glutaraldehyde at pH 3.2. In this experiment the 1331 pulse sequence ('water-suppression' technique) was applied[10], with time parameters set to optimize the intensity at the chemical shift resonance of the aldehyde protons. At the start of the reaction a fine structure (triplet) is evident which is caused by the coupling of the aldehyde proton to the nearest methylene protons. As the reaction proceeds this fine structure seems to disappear. The reason for this is probably related to the increasing viscosity of the solution, which in turn affects the linewidth of the peak, i.e. the linewidth becomes significantly larger than the coupling constant and causes a suppression of the spectral details. The numerical values of the peak intensity (area) *versus* time are shown in *Figure 4*. Two additional decay curves are shown for the same gel system at 84 and 101°C, respectively. The solid curves in *Figure 4* represent non-linear least squares fit of equation (1a) to the observed data, where I represents the signal intensity at time t; C_0 is a constant and k represents the decay rate.

$$I(t) = C_0 \exp(-k \cdot t) \tag{1a}$$

Alternatively, expressed as

$$k = \frac{\ln C_0 - \ln I(t)}{t} \tag{1b}$$

The observed decrease in intensity *versus* time of the aldehyde peak is faster with increasing temperature, as expected. The same system has been studied under different conditions, i.e. by varying the pH, the temperature and the dialdehyde concentration. The results are summarized in *Table 1*. From the estimated decay rates derived at different temperatures (*Figure 4*) the activation energy (ΔE) is estimated by assuming that the decay rate follows an Arrhenius type of behaviour, i.e.

$$k = \nu_0 \exp(-\Delta E/RT) \tag{2}$$

where ν_0 is the pre-exponential factor, R is the gas constant, and T is the absolute temperature. The activation energies determined by equation (2) are summarized in *Table 2*.

Table 1 Decay rates, equation (1), of the aldehyde peak *versus* pH and aldehyde concentration (C_x). The PVA concentration was kept constant at 2 wt%

System	Temp (°C)	C_x (mM)	pH	$k \cdot 10^5$ (s^{-1}) (calculated)[a]	$k \cdot 10^5$ (s^{-1}) (observed)[b]
I	72	5	3.2	10.8	13.1 ± 0.7
I	84	5	3.2	20.0	19.7 ± 0.8
I	101	5	3.2	45.3	38 ± 2
IIa	61	10	3.2	12.5	10.3 ± 0.8
IIa	72	10	3.2	23.7	26 ± 2
IIa	84	10	3.2	44.1	48 ± 2
IIb	84	5	4.7	1.2	1.07 ± 0.02
IIb	93	5	4.7	1.9	1.84 ± 0.05
IIb	101	5	4.7	2.7	3.0 ± 0.5

[a] Calculated from equation (4b)
[b] Fitted to equation (1b)

A simplified reaction scheme of the dialdehyde species (C) during the gelation process with PVA is schematically represented in *Scheme 1*. In *Scheme 1*, L_1 and L_1' represent PVA–aldehyde bonds through hemiacetal and acetal proper, respectively. L_2, L_2' and L_2'' represent crosslinks between PVA and the former dialdehyde, through dihemiacetal, acetal–hemiacetal and diacetal, respectively; i.e. PVA–aldehyde–PVA crosslinks. The three latter species are responsible for the gelation reaction. In principle, all the hemiacetal and acetal proper species (L_n) should give rise to proton resonance peaks at approximately 4.7 ppm. However, this is too close to the resonance peak of the solvent water protons and will thus not be observable due to the solvent water suppression technique applied. A simple single pulse sequence was also tried out, but the intensity of the methine proton was too small compared to the intensity of the water protons (1 : 20 000) to be observable due to the limited number of bits (12) in the ADC.

From the reaction illustrated in *Scheme 1*, only the overall rate k_d for the formation of PVA–aldehyde hemiacetal links can be derived. The transformation from hemiacetal to acetal proper, k_2, k_5, k_6, and the reverse reactions will be invisible to the applied technique.

$$k_d = k_1 + k_3 + k_4 \tag{3}$$

The decay rate k_d of the aldehyde proton as given in equation (3) can be reformulated into a more general expression of the form:

$$k_d = k \cdot C_x^{\alpha} \cdot C_{H^+}^{\beta} \cdot C_p^{\gamma} \cdot \exp(-E/T) \tag{4a}$$

where C_x is the aldehyde concentration, C_p is the PVA concentration, and C_{H^+} represents the acidity of the solution. E and k are constant parameters, and the parameters α, β and γ represent the reaction orders with respect to each of the reactants. Since the concentration of PVA is constant and much higher than that of the other reactants, equation (4a) can be simplified further to give

$$k_d = k' \cdot C_x^{\alpha} \cdot C_{H^+}^{\beta} \cdot \exp(-E/T) \tag{4b}$$

the term C_p^{γ} in equation (4a) is included in the parameter k'. Equation (4b) is fitted to the observed data presented in *Table 1* using a linear-programming technique[12], which iteratively solves a set of linear equations in a finite number of steps if a solution exists, or otherwise indicates an unbounded solution. The results of this analysis give $k' = 2.00 \times 10^6\ s^{-1}$, $\alpha = 1.138$, $\beta = 0.821$ and $E = 15.46$ K. The decay rates (k_d) calculated from equation (4b) are shown in *Table 1* and are in good agreement with the corresponding decay rates derived from equation (1). An interesting conclusion is that the reaction order with respect to the aldehyde concentration and the H^+ concentration is approximately unity. However, we should keep in mind that the monomer aldehyde concentration is dependent on temperature, which—as discussed previously—can be significantly smaller than the nominal aldehyde concentration C_x.

Table 2 Activation energies for Systems I–IIa in *Table 1* as determined from equation (2)

System	ΔE (kJ mol^{-1})
I	40.5 ± 1.2
IIa	62 ± 7
IIb	66.3 ± 0.5

PVA and DHF

Figure 5, shows the ^{13}C and ^{1}H n.m.r. spectra of pure DHF—the structure of which is shown schematically in *Scheme 2*—at room temperature.

The ^{13}C n.m.r. spectrum was run without NOE using proton decoupling only during acquisition. A short pulse angle (5°) and a long repetition time of 60 s assured

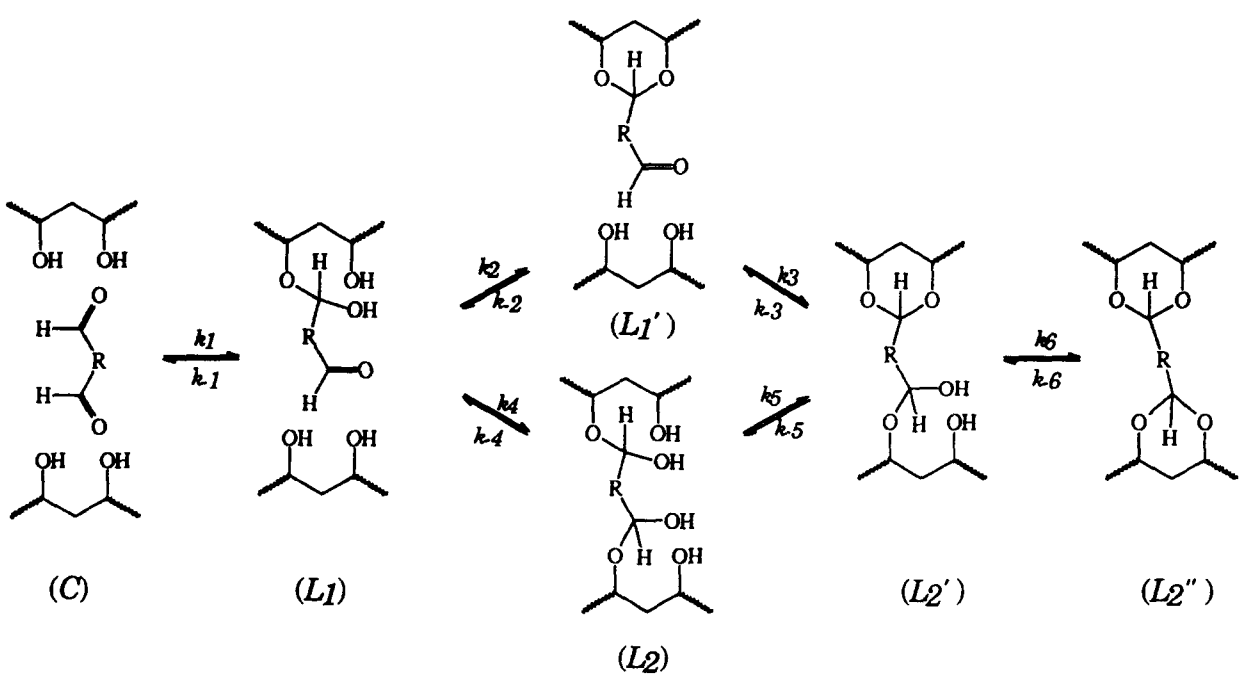

Scheme 1

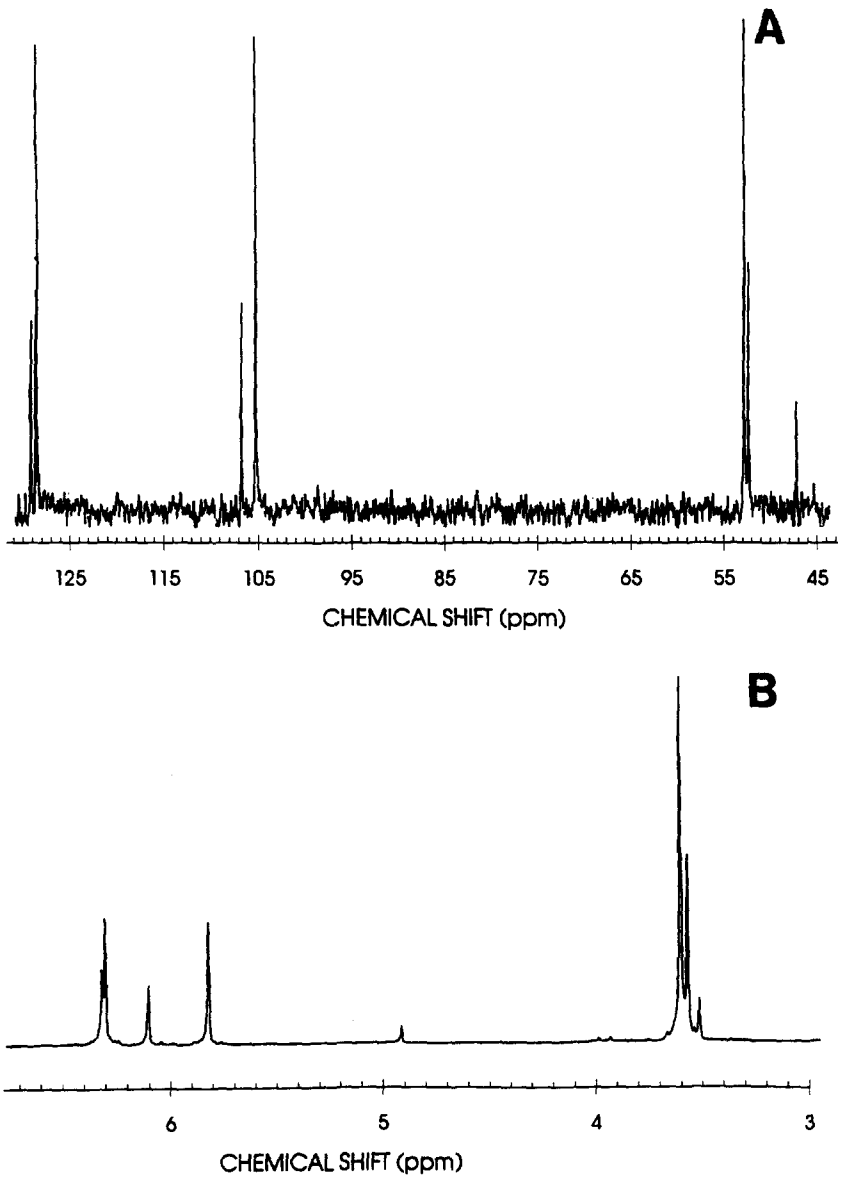

Figure 5 (A) ^{13}C n.m.r. and (B) ^{1}H n.m.r. spectra of (DHF) at room temperature and pH 3.5. See text for further details

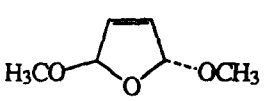

(DHF)

Scheme 2

quantitative sampling of the spectrum. A DEPT[13] spectrum (not shown) gave uniquely the number of directly coupled protons on each carbon nucleus. The spectrum shows seven peaks, which are due to the *cis* and *trans* isomers of DHF. The smaller resonance line at approximately 50 ppm was assigned to the methyl carbon in methanol, subsequently verified by addition of methanol to the solution. The other six resonance lines in the spectrum can be divided into two groups composed of three lines each, corresponding to the *cis* and *trans* isomers of DHF. The olefin carbon resonates at 129 ppm and the methine carbon resonates at 107 ppm. The resonance peaks at approximately 53 ppm correspond to the methyl carbons in the methoxyl groups. The ratio of isomers was found to be approximately 1/2. The three resonance peaks around 3.6 ppm in the ^{1}H n.m.r. spectrum (*Figure 5b*) correspond to—from high to low field—the methyl protons on the methanol and methoxyl protons in *cis*- and *trans*-DHF. The resonance peaks in the range 5.8–6.4 ppm correspond to the olefin protons and the methine protons in the DHF structure, respectively. These four residual protons in the DHF structure constitute an AA′BB′-spin system and renders the ^{1}H n.m.r. spectrum somewhat more difficult to assign. A more detailed identification/assignment of these peaks was of minor concern and is not discussed any further in this work. Of particular importance is the rather small peak at approximately 10 ppm (not shown) which is the aldehyde resonance peak. According to the assumed reaction (*Scheme 3*), where *B* represents the aldehyde (*Z*-butenedial), the intensity of *B* is expected to be approximately 1/3 the intensity of the methyl peak of methanol. However, the intensity of this peak was significantly smaller than 1/3, which might be due to hydration of the aldehyde group in the acidic solvent.

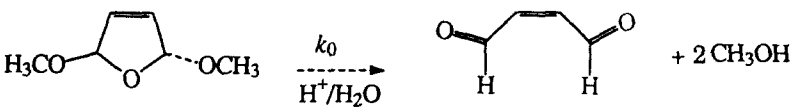

(DHF) (*B*)

Scheme 3

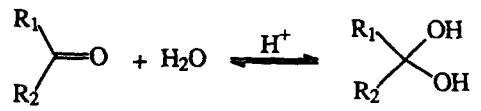

Scheme 4

The equilibrium reaction illustrated in *Scheme 4* will yield a significant concentration of the hydrated species; the equilibrium constants K are reported[14] for K ($R_1 = CH_3$; $R_2 = H$) $= 1.4 \times 10^3$ and K ($R_1 = R_2 = H$) $= 2 \times 10^3$.

PVA dissolved in water at pH < 7 forms a gel when adding small amounts of DHF[15]. We tentatively believe that the gelation process is connected with the cross-linking of the dialdehyde formed in *Scheme 3* with PVA as illustrated in the generalized *Scheme 1*, outlined for this system in *Scheme 5*.

In *Scheme 5*, G_1 is short-hand notation for the concentration of PVA–*B* links through a hemiacetal, and G_2'' represents the *B*–PVA–*B* crosslinks through acetal proper. Moreover, butenedial (*B*) will hydrolyse reversibly to give *B'* and *B''*, as illustrated in *Scheme 6*. Aldehydes in aqueous solution are known to produce polymeric species reversibly; these will, however, not be included in this discussion.

Thus, the overall reaction of the formation of PVA–*B* hemiacetal bonds (G_1) and acetal proper bonds (G_2) can be illustrated by the simplified reaction scheme in *Scheme 7*, only considering one half of the dialdehyde, where *D* is short-hand notation for DHF. As discussed above, only overall rates can be deduced by the employed method, so *Scheme 7* may be simplified down to the scheme shown in *Scheme 8*.

The rate k_2' will be the overall rate of formation of acetal entities. From *Scheme 8*, the following set of rate equations can be deduced:

$$\begin{aligned} \frac{dD}{dt} &= k_0 D \\ \frac{dB}{dt} &= k_0 D - k_2' B - k_h B + k_{-h} B' \\ \frac{dB'}{dt} &= k_h B - k_{-h} B' \\ \frac{dG_2}{dt} &= k_2' B \end{aligned} \tag{5}$$

Throughout the reaction, the concentration of *B* is very small. Assuming, therefore, *B* to be in steady state ($dB/dt = 0$) and *B* and *B'* to be in equilibrium ($dB'/dt = 0$), the following equations are derived:

$$\frac{dG_2}{dt} = -\frac{dD}{dt} \tag{6}$$

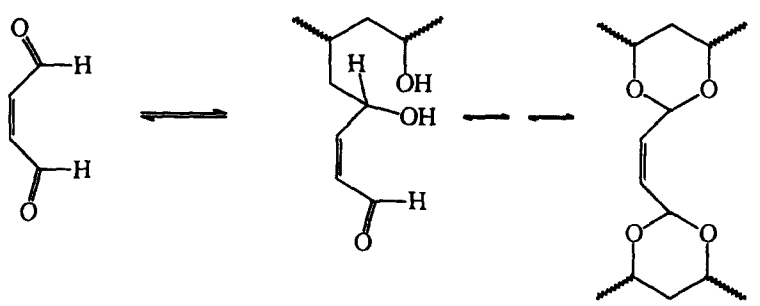

(*B*) (*G*1) (*G*2'')

Scheme 5

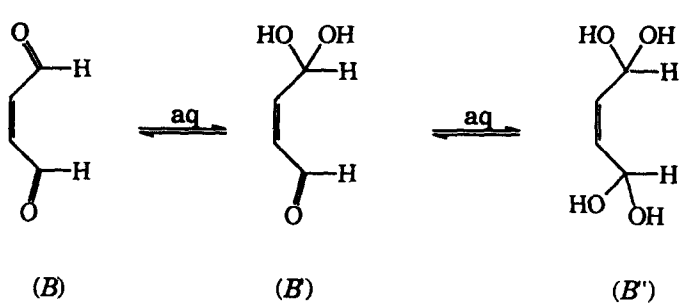

(*B*) (*B'*) (*B''*)

Scheme 6

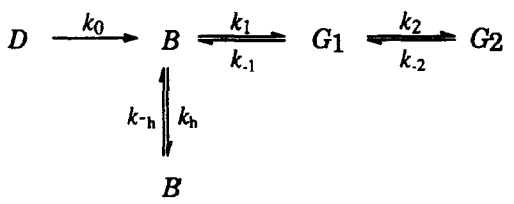

Scheme 7

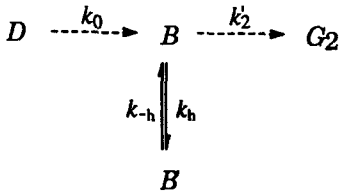

Scheme 8

$$G_2 = D_0(1 - e^{k_0 t}) \quad (7)$$

suggesting that the rate of formation of PVA–*B* links (i.e. dG_2/dt) is equal to the rate of consumption of DHF (i.e. dD/dt). The characteristic peaks for DHF in the ^{1}H n.m.r. spectrum is found in the chemical shift range 5.7–6.5 ppm. *Figure 6* shows the time dependency of the methine resonance peak intensity (=CH-CH-OCH_3) during reaction of System I at 101°C (*Table 3*). The numerical data for the intensity *versus* reaction time for System I at three different temperatures are illustrated in *Figure 7*. The solid curves represent non-linear least squares fits of a single exponential function, equation (1b), to the observed data. The effect of the DHF concentration on the decay rate was investigated by doubling the concentration of DHF. The results are shown in *Tables 3* and *4* and suggest that the observed decay rates and activation energies are not affected—within experimental error—by doubling the DHF concentration. The decay rates of two identical systems (Systems IIa and IIb) were determined and show reasonably good reproducibility (*Table 3*). We have—at present—no reasonable explanation for this lack of sensitivity in activation energies and decay rates with changing DHF concentration. Note that from the decay rate of the dialdehyde peak, only the rate of formation of PVA–*B* links (G_1) is derived and not the formation rate of crosslinks (*B*–PVA–*B*). This crosslinking reaction would follow as a reversible reaction from G_2 in *Scheme 8*. This means that the rate of gelation remains undetermined. In order to estimate the reaction rate of this latter reaction step, other peaks belonging to the aldehyde proton or acetal proton should be followed *versus* time.

The acetal peak was, unfortunately, masked by other and more dominant peaks in the spectrum and was not amenable for detection. However, for one of the systems (System I; *Tables 3* and *4*) it was possible to follow the growth and later decay of the low ^{1}H n.m.r. intensity of the aldehyde proton *versus* reaction time and temperature, as depicted in *Figure 8*. This observation is rationalized according to the reaction model presented in *Scheme 8* by implicitly making one single assumption: that *B* is in equilibrium with *B'* at any time during the reaction (i.e. $dB'/dt = 0$). Solving equation (5) under this assumption gives

$$B = D_0 \cdot \frac{k_2'}{k_2' - k_0}[e^{-k_0 t} - e^{-k_2' t}] \quad (8)$$

$$G_2 = D_0\left\{\frac{k_2'}{k_0 - k_2'} \cdot e^{-k_0 t} - \frac{k_0}{k_0 - k_2'} \cdot e^{-k_2' t} + 1\right\} \quad (9)$$

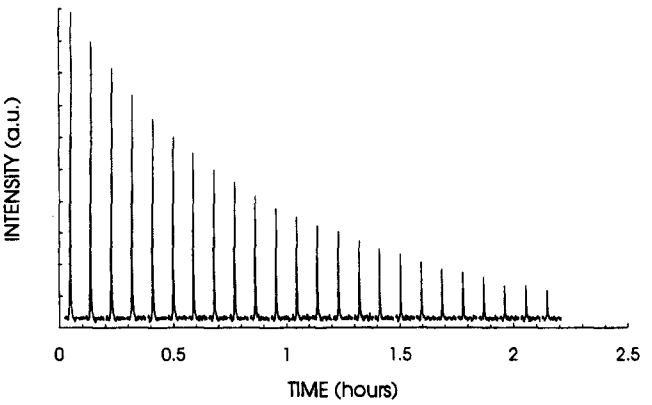

Figure 6 ^{1}H n.m.r. spectra of the methine proton resonance in DHF *versus* reaction time at 95°C of a 2 wt% PVA + 5 mM DHF solution at pH = 3.2 (System I)

Table 3 Decay rates of the methine resonance peak in DHF *versus* pH and DHF concentration (C_x). The PVA concentration is kept constant at 2 wt%

System	Temp (°C)	C_x (mM)	pH	$k \cdot 10^5$ (s^{-1}) (observed)
I	84	5	3.2	8.8 ± 0.3
I	93	5	3.2	18.0 ± 0.4
I	101	5	3.2	29.8 ± 1.6
IIa	84	10	3.2	8.9 ± 0.2
IIa	93	10	3.2	18.4 ± 0.7
IIa	101	10	3.2	40.5 ± 2.8
IIb	93	10	3.2	18.7 ± 0.3
IIb	101	10	3.2	35.4 ± 0.6

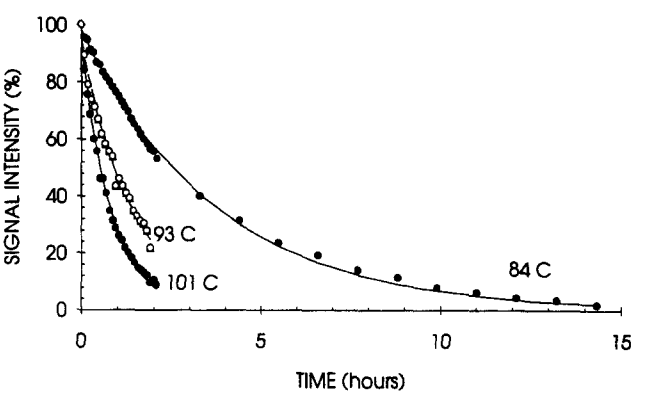

Figure 7 Intensity (area) of DHF *versus* time of a 2 wt% PVA + 5 mM DHF aqueous solution at pH 3.2 (System I) at three different temperatures. The temperatures are in °C

Table 4 Activation energies for Systems I–IIa in *Table 3* as determined from equation (2)

System	ΔE (kJ mol^{-1})
I	74 ± 10
IIa	96 ± 10

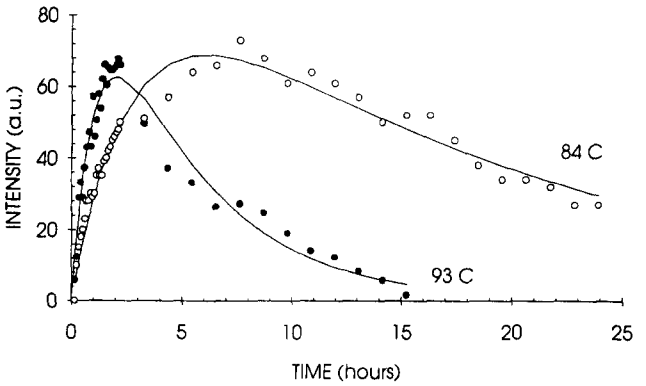

Figure 8 Intensity (area) of the dialdehyde peak (butadiene) *versus* time of a 2 wt% PVA + 5 mM DHF solution at pH 3.2 (System I) at two different temperatures

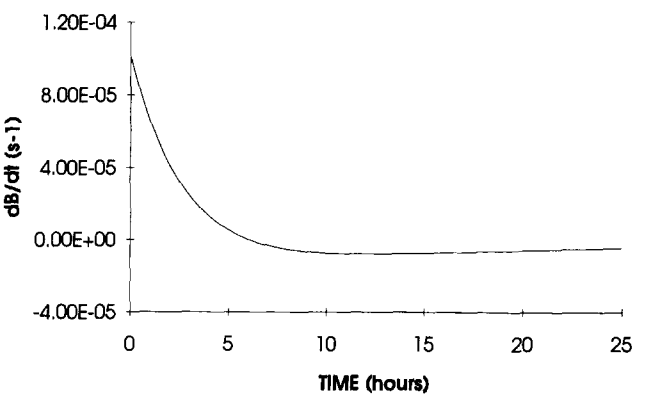

Figure 9 Change of aldehyde concentration (i.e. signal) dB/dt *versus* time for System I

The solid lines in *Figure 8* represent non-linear least squares fits to the observed data points and give $k_0(84°C) = (10.1 \pm 0.8) \times 10^{-5} s^{-1}$, $k'_2(84°C) = (1.57 \pm 0.15) \times 10^{-5} s^{-1}$, $k_0(93°C) = (25.7 \pm 3.3) \times 10^{-5} s^{-1}$ and $k'_2(93°C) = (6.04 \pm 0.68) \times 10^{-5} s^{-1}$. The first of these two decay rates (k_0) is similar in magnitude to the decay rate observed for the 'consumption' of DHF when assuming steady-state conditions of the butenedial concentration (B). However, the latter experimental data indicate that the hypothesis of a steady-state condition with respect to the dialdehyde concentration is a rather poor assumption early in the reaction, as can be seen from comparison after insertion of experimental values into equations (8) and (9). An illustration of the time development of dB/dt is shown in *Figure 9*.

The rate of formation (k'_2) of PVA–aldehyde links (L_1 and L_2) is five times slower than the formation of the aldehyde. Moreover, the activation energies for the first and second reaction steps of *Scheme 8* are approximately identical and of the same size as previously determined.

One observation which confuses us is the complete disappearance of resonance lines in the shift range, 5.7–6.5 ppm during the reaction, suggesting that the double bond in DHF breaks down as well. Additional work is necessary to pin down the details concerning the reaction mechanisms of the gelation process. This is, however, not the topic of this work.

CONCLUSIONS

The n.m.r. studies of the reaction between PVA and dialdehyde crosslinkers have shown that this technique is a useful tool for studies of the reaction kinetics during gel formation. The reaction between PVA and dialdehyde has been studied as a function of temperature, pH and dialdehyde concentration, variables of importance for practical use when forming gel with this system in an oil reservoir. However, it must be stressed that this paper only describes initial n.m.r. studies of the reaction between PVA and dialdehyde, and more work is needed in order to describe this system more rigorously.

The reaction of PVA and glutaraldehyde (G) suggests that the first step towards the formation of crosslinks between PVA and G goes through the intermediate formation of PVA–G bonds. The rate of this reaction is found to be of approximately first order with respect to both the H^+ concentration and the formal dialdehyde concentration. The activation energy increases with increasing dialdehyde concentration and pH (3.2–4.7). The rate of formation of crosslinks (PVA–G–PVA) would be identical to the formation of PVA-G links if these latter species were assumed to be in a steady state during the reaction. However, this is probably a very crude assumption. Due to a severe overlap of peaks in the ^1H n.m.r. spectra, the resonance peaks corresponding to formation of hemiacetals and acetals could not be detected, making a direct measurement of the rate of gel formation (k_4) difficult if not impossible.

Likewise, the ratio of formation of PVA–aldehyde bonds in the PVA–DHF system could be derived from the observed decay rate of butenedial *versus* reaction time. This rate was found to be approximately an order of magnitude slower (at 84°C) than the corresponding rate of formation of PVA–aldehyde bonds in the PVA–glutaraldehyde system. Also, the activation energy of formation of PVA–aldehyde bonds was approximately 50% larger in the PVA–DHF system compared to that the PVA–glutaraldehyde system.

ACKNOWLEDGEMENTS

This work has been supported by the Research Council of Norway, BP Norway, Norske Shell, Norsk Hydro, Statoil, Saga Petroleum and Total Norge as a part of the RUTH research programme.

REFERENCES

1. Stahl, G. A. and Schulz, D. N. (eds), *Water Soluble Polymers for Petroleum Recovery*. Plenum Press, New York, 1988, p. 299.
2. Tackett, J. E., US Patent No. 5 069 281, 1991.
3. Olafsen, K., Hansen, E. W., Hustoft, A. G., Jahr, D. M. and Stori, A., in *PROFIT Project Summary Report*, ed. J. Olsen, S. Olaussen, T. B. Jensen, G. H. Landa and L. Hinderaker. Norwegian Petroleum Directorate, Stavanger, 1995, p. 247.
4. Prud'homme, R. K. and Uhl, J. T., SPE/DOE 12640, 1984.
5. DiGiacomo, P. M. and Schramm, C. M., SPE 11787, 1983.
6. Tackett, J. E., *J. Appl. Spec.*, 1991, **45**, 1674.
7. Hansen, E. W. and Lund, T., *J. Phys. Chem.*, 1991, **95**, 341.
8. Hansen, E. W. and Lund, T., *J. Phys. Chem.*, 1995, **99**, 9811.
9. Shaw, D., in *Fourier Transform NMR Spectroscopy*. Elsevier Scientific, Amsterdam, 1976, p. 149.
10. Hore, P. J., *J. Magn. Res.*, 1983, **55**, 283.
11. Roberts, J. D. and Caserio, M. C., in *Basic Principles of Chemistry*, 2nd edn. W. A. Benjamin Inc., Menlo Park, CA, 1977, p. 696.
12. Danzig, G., in *Activity Analysis of Production and Allocation*, ed. T. C. Koopman. Wiley, New York, 1951.
13. Bovey, F. A., in *Nuclear Magnetic Resonance Spectroscopy*, 2nd edn. Academic Press, London, 1988, pp. 245–250.

14. Sykes, P., in *A Guidebook to Mechanism in Organic Chemistry*, 6th edn. Longman Scientific and Technical, Harlow, 1986, 209.
15. Olafsen, K., Hansen, E. W., Holm, K. H., Jahr, D. M. and Stori, A., in *RUTH Program Summary*, ed. S. M. Skjæveland, A. Skauge, L. Hinderaker and C. D. Sisk. Norwegian Petroleum Directorate, Stavanger, 1996, p. 275.